EFFECTS OF STRESS ON MAGNETIC FLUX LEAKAGE AND MAGNETIC BARKHAUSEN NOISE SIGNALS

D.L. Atherton, T.W. Krause and K. Mandal
Applied Magnetics Group, Department of Physics
Queen's University, Kingston, ON., K7L 3N6, Canada

INTRODUCTION

Pipelines are pressure vessels. Their enviable safety record compares well with other transportation modes. Typical pipeline fatality rates are about 1% those of rail or air which are, in turn, about 1% of highway fatalities. Pipeline safety is first assured by rigorous inspection during pipe manufacture and line construction. All welds are inspected using radiography to detect voids and ultrasonics to sense cracks. Oil and gas transmission lines are normally buried, so in service inspection must be performed from the inside by pumping an inspection "pig" through the line. Magnetic flux leakage (MFL) pigs are the most cost effective tools for corrosion monitoring. They are propelled by differential product pressure from one compressor or pumping station to the next, which may be more than 100km away. They are self supporting, demand maximum data storage density and highest energy storage battery power supplies as well as advanced signal processing to obtain signal discrimination and data compression.

An MFL inspection pig contains a circumferential array of MFL detectors using high strength NdFeB permanent magnets to magnetize the pipe wall to near saturation flux density [1]. Anomalies in the pipe wall, such as corrosion pits, result in anomalous magnetic leakage flux near the inner and outer surfaces of the pipe. These anomalous leakage fluxes are detected by small Hall probes or induction coils moving with the MFL detector. High resolution MFL tools are now common. Skill is required to interpret their high resolution records to give precision defect sizing needed for calculating safe maximum allowable operation pressures or for monitoring remedial or protective action, such as cathodic protection.

Four factors govern MFL signal patterns. These are:

1) Defect geometry - obviously! - and position (near or far side).
2) MFL tool design - length, pipe wall flux density, fringing fields, etc.
3) Running conditions - velocity, line pressure [2], pipe conditions, etc.
4) Magnetic properties of the pipe, particularly anisotropy and uniformity - These are unrelated to API grade or mechanical specifications. They also depend on residual stresses generated by steel rolling, pipe forming, mechanical or hydrostatic post expansion or testing, cold field bending, etc.

Review of Progress in Quantitative Nondestructive Evaluation, Vol. 16
Edited by D.O. Thompson and D.E. Chimenti, Plenum Press, New York, 1997

Line pressure, bending and residual stresses can have large effects on the magnetic properties of line pipe steels [3]. Line pressure can alter MFL signal amplitudes by as much as 80%. Corrections for stress effects must be applied to high resolution MFL inspection logs in order to size defects accurately. Therefore details of the magnetic properties and the complex effects of stress on the particular line pipe must be studied. Here we describe the effects of line pressure and bending stresses and the consequent stress-induced changes in magnetic anisotropy on MFL patterns from simulated corrosion pits in samples of Gas Research Institute's pipeline simulation facility flow test loop. The simulated pits used here are typically 13mm diameter, 50% penetration, ball-milled, round-bottomed blind holes. The pipe samples are 610mm diameter, 9mm wall API X70 line pipe with a nominal yield strength of 480MPa.

We have built many special rigs for testing the effects of line pressure, bending and residual stress on the magnetic properties of line pipe steels and on MFL patterns. The ones used for this work are a hydraulic pressure vessel used to simulate line pressure and a composite beam bending rig used to simulate pipe bending. The hydraulic rig is shown in Fig. 1. A short test pipe encircles a flanged spool piece to which it is sealed by compressed O rings. The intervening space is pressurized hydraulically. This minimizes and decouples end forces from the test section which experiences only circumferential tensile hoop stresses. Pressures up to 100bar have been used to stress the pipe to 70% of yield strength. The composite beam rig, shown in Fig. 2, applies bending stress to a truss beam formed of two long narrow axial strips cut from the test pipe and separated by a web of epoxy bonded, laminated high strength fibreglass wood strips. The composite beam is designed to generate nearly constant tension or compression in the outer test strip, simulating the effect of pipe bending. In both cases the MFL detectors generate axial magnetic fields which are applied after stressing to simulate an MFL inspection tool pumped through a pressurized or bent pipe.

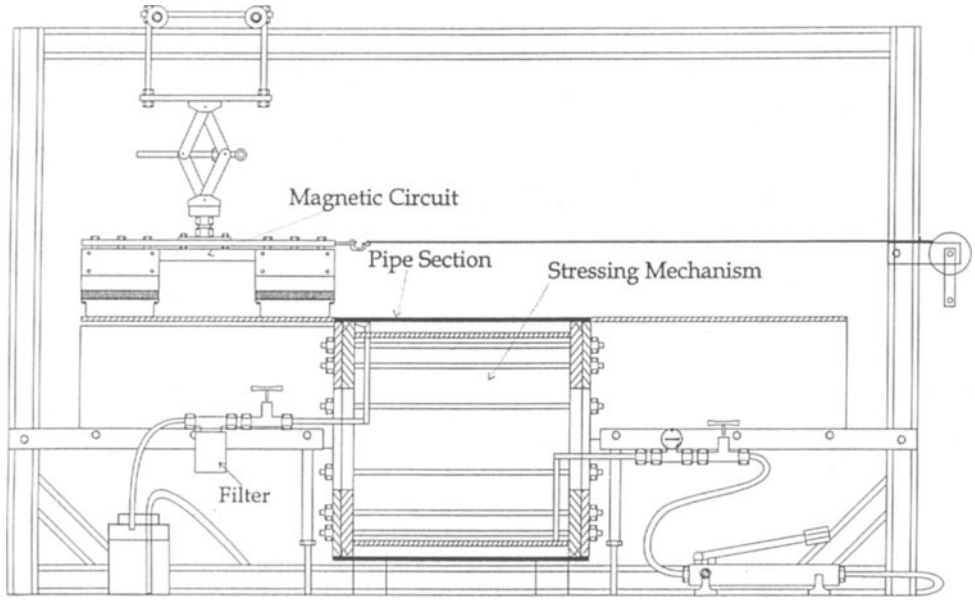

Fig. 1. Hydraulic rig for simulating line pressure stress. The MFL detector is pulled onto the pipe and the MFL pattern mapped. The MFL is then pulled off the opposite end, lifted and returned to the start before the pressure is changed.

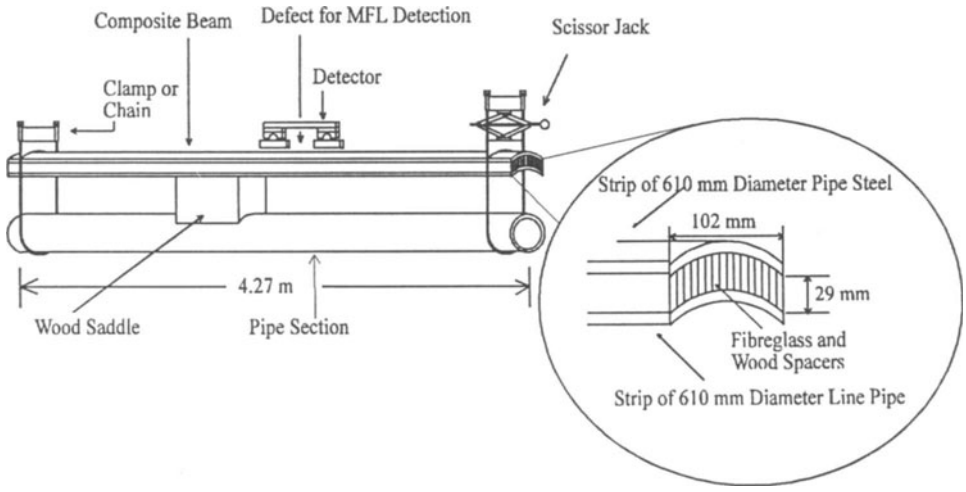

Fig. 2. Composite beam bending apparatus used to produce axial bending stress.

The narrow strips used in the composite beam test rig limit circumferential flux spreading but guard detectors are used on the hydraulic test rig. Several different magnetizer configurations have been used to give a range of pipe wall flux densities. These are initially estimated from MFL signals and subsequently calibrated using flux coils threaded through the composite beam to enclose the test strip or threaded through the outer test wall of the hydraulic pressure vessel.

MFL TEST RESULTS AND DISCUSSION

Precision maps of all three components of the MFL near side defects are measured and recorded using a simple computer-controlled two axis stepper motor system to scan a small Hall probe over the outer surface of the pipe. Typical step sizes are 1mm. Fig. 3 shows examples of surface and contour plots of the MFL radial component measured above a simulated near side corrosion pit in the composite beam with and without applied axial tensile bending stress. Here stress causes an increase in the peak-to-peak MFL signal amplitude (MFL_{pp}) and also a change in the pattern. The latter effect is attributed to surface effects and are normally only observed for near side defects [4]. Fig. 4 shows examples of MFL_{pp} increases with stress for different flux densities for a near side pit, measured on the composite beam where the bending stress is aligned with the axial field. Similar measurements for pits on the hydraulic pressure vessel show MFL_{pp} signals decreasing with stress, but the line pressure stress is then orthogonal to the axial field. The changes depend on the pipe wall flux density and can be large, even at high flux densities. Furthermore the stress-induced changes in MFL signals depend on the initial magnetic properties of the line pipe, which may vary over just a few mm. This is evident from Fig. 5 which compares stress-induced changes in MFL_{pp} between near and far side pits for stresses parallel and perpendicular to the field (composite beam and hydraulic pressure vessel rigs respectively). Surprisingly, the far side pits show greater stress sensitivities. This is due to the difference in the magnetic properties on the inside and outside of the pipe, particularly differences in magnetic anisotropy. The MFL_{pp} variations are caused by stress-induced changes in bulk magnetic anisotropy, including easy axis of magnetization [5], and also local changes in anisotropy in the region of defects due to their acting as stress raisers. Changes in bulk magnetic anisotropy affect primarily the MFL_{pp} signal amplitude.

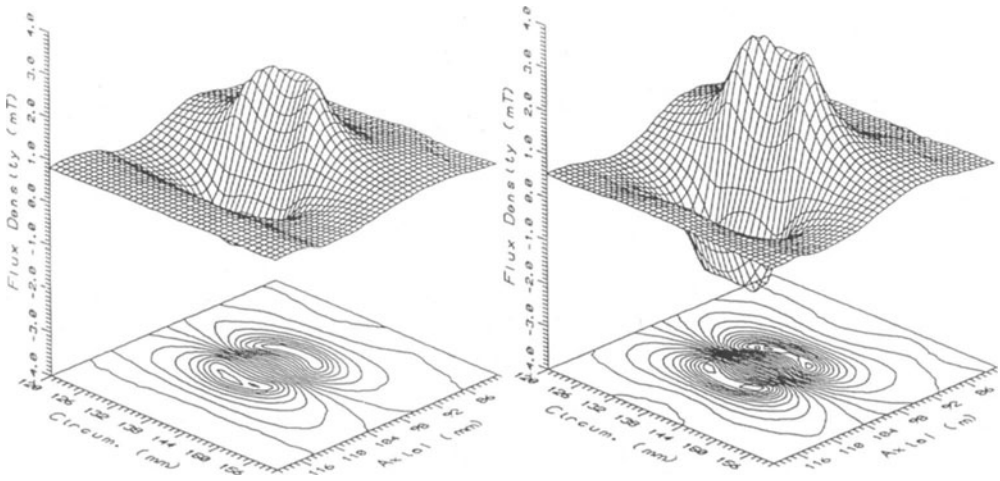

Fig. 3. Surface and contour plots of radial MFL from near side pit at 1.2T axial flux density at 0 applied stress (left) and 340MPa axial tensile stress (right).

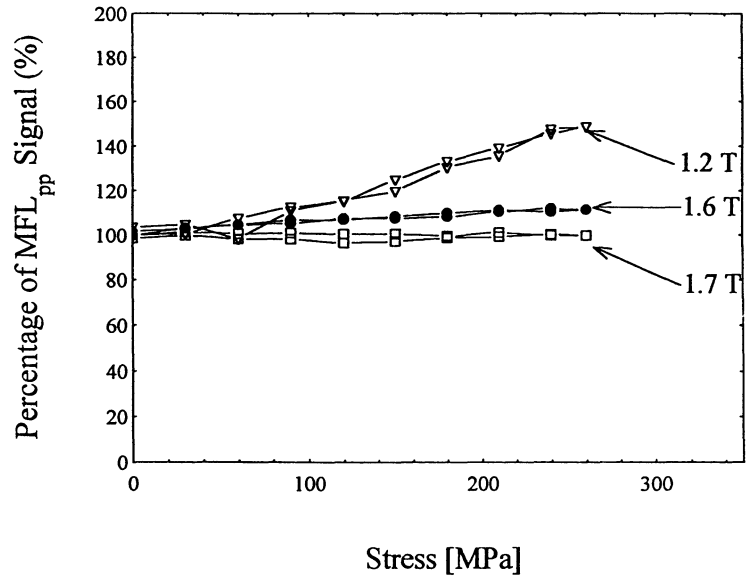

Fig. 4. Percentage radial MFL_{pp} signal with respect to 0MPa as functions of stress, at various flux densities, for near side electrochemically pit on the composite beam.

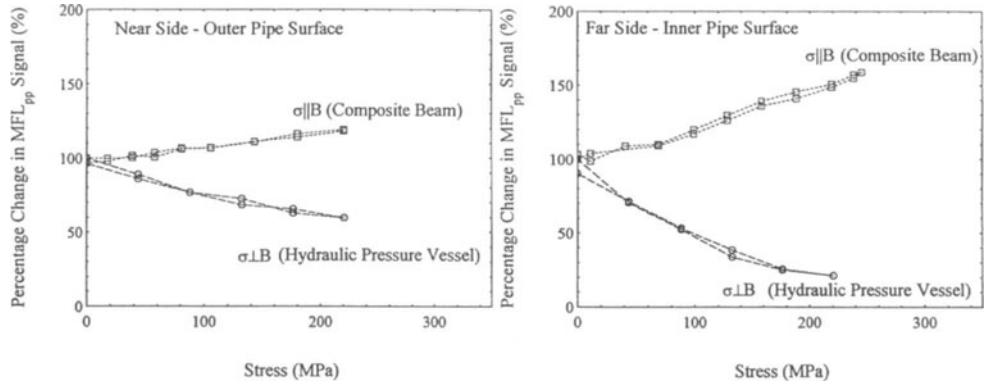

Fig. 5. Percentages of radial MFL_{pp} with respect to 0MPa MFL_{pp} as functions of stress for near (left) and far (right) side pits measured at 1.1T axial flux density for parallel (composite beam) and orthogonal (hydraulic pressure vessel) stresses.

In steel, which has positive magnetostriction, tensile stress tends to swing the easy axis of magnetization toward the stress direction, whilst compressive stress tends to swing the easy axis away from the stress direction. Changes in MFL signal patterns, such as the double peak feature, are attributed primarily to surface changes in local anisotropy near the defect and are normally observed only for near side defects. It is clear that the initial easy axis direction and amount of anisotropy are important. These are determined by such factors as preferred crystalline orientation and residual stresses. It is particularly difficult to measure magnetic anisotropy nondestructively but we have developed magnetic Barkhausen noise (MBN) techniques to monitor stress-induced changes in surface magnetic anisotropy and also magnetic uniformity.

MAGNETIC BARKHAUSEN NOISE (MBN) MEASUREMENTS

When a smoothly increasing field is applied to a ferromagnetic material its magnetization increases in small discontinuous jumps due to domain walls being driven across pinning sites. The irregular magnetization changes can be sensed by magnetic coils on the surface or encircling the ferromagnet or acoustically. Fig. 6 shows a schematic of apparatus for surface MBN anisotropy measurements. It consists of a small U core electromagnet energised with 12Hz AC. Between the

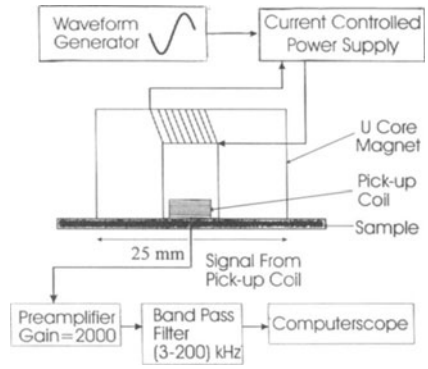

Fig. 6. Magnetic Barkhausen noise apparatus for monitoring magnetic anisotropy.

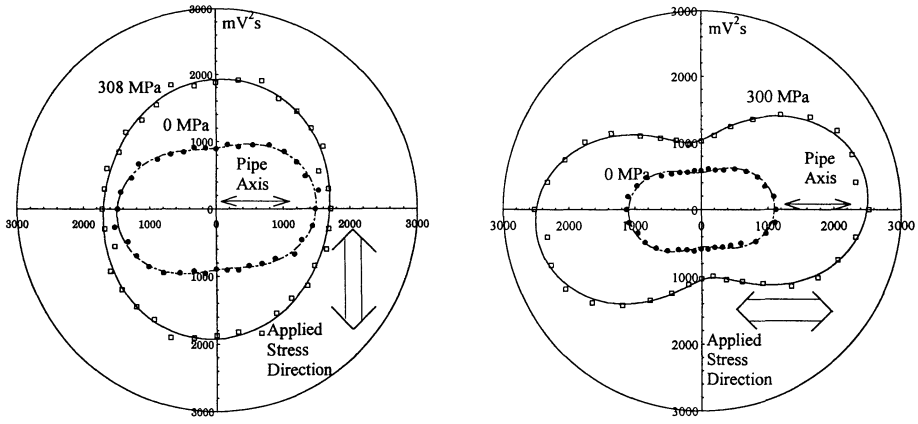

Fig. 7. Angular dependent MBN_{ENERGY} signal at 0 and 300MPa tensile stress on the outside surface using the hydraulic pressure vessel (left) to generate stress orthogonal to pipe axis and the composite beam (right) generating uniaxial stress.

pole pieces is a miniature pancake coil whose output is connected through a preamplifier and bandpass filter to a PC based data acquisition and processing system (computerscope). MBN signals can be processed in many ways. We integrate the square of the voltages above a small threshold over eight cycles to obtain an MBN_{ENERGY} signal. This can be measured as a function of sweep field angle. Fig. 7 shows examples of polar plots of these MBN_{ENERGY} signals with and without applied uniaxial and perpendicular stresses. The longer axes of the contours indicate the magnetic easy axis and the eccentricity the anisotropy. The contours can be fitted by the model-based relationship containing isotropic and angularly dependent terms [6]. The symbols are defined in Fig. 8.

$$MBN_{ENERGY} = \alpha \cos^2(\theta-\phi) + \beta \quad (1)$$

The effects of stress are described by an MBN_{ENERGY} ratio defined as the MBN_{ENERGY} signal in the axial MFL exciting field direction to that in the

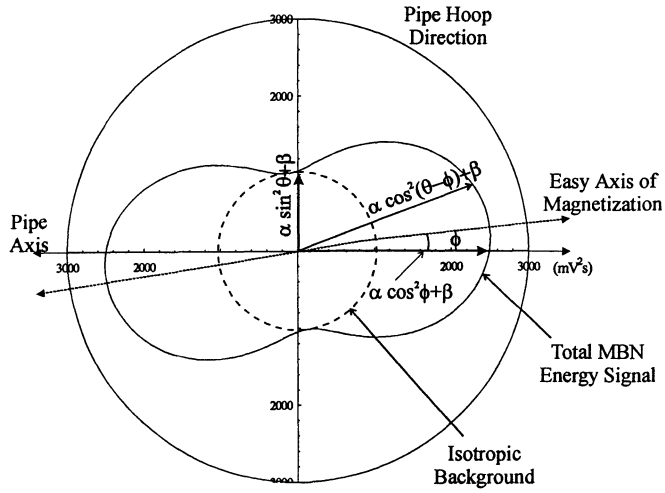

Fig. 8. Parameters used to define the MBN_{ENERGY} ratio as the MBN_{ENERGY} signal in the axial MFL exciting field direction to the signal in the orthogonal direction.

orthogonal direction. This varies with stress due to the changing magnetic easy axis direction and the ratio of isotropic and angularly dependent noise contributions.

CORRELATION OF MBN_{ENERGY} RATIO AND MFL_{PP} SIGNAL VARIATIONS

Fig. 9 shows examples of MBN_{ENERGY} ratio and MFL_{pp} signal variations for various flux densities with stress. There is a generally good correlation between the MBN_{ENERGY} ratio and MFL_{pp} signals for low flux densities (the 1.1-1.2T region). This is because they are both influenced by stress-induced changes in magnetic anisotropy, however the MBN emission is most intense near the mid field knee of the magnetization curve. MFL inspection tools aim to use high flux densities partly because this tends to reduce the stress-induced changes in MFL signals, as shown in Fig. 10, but it must be noted that this depends on the initial magnetic properties of the particular line pipe. Better high field correlations are therefore needed. Fig. 11 shows polar plots of MBN_{ENERGY} for mid and high fields obtained by dividing the MBN emissions into different field regions. As expected, there appears to be less anisotropy at high fields. There are however several further problems which we are addressing: This separation is in terms of magnetizing H field whereas what is more appropriate is flux density, B. MBN at high flux densities is relatively small, largely because high field magnetization mechanisms are principally magnetization rotations. A further limitation is that this nondestructive MBN measurement monitors anisotropy only in the surface. It would be desirable to measure the total through-wall anisotropy and also anisotropy in the radial direction.

CONCLUSIONS

The effects of line pressure and other stresses on MFL signals are complex. They can be large, even at high flux density, so corrections may be needed to enable the highest precision in defect sizing. The effects result from stress-induced changes in bulk and local anisotropies and depend on the particular line pipe. Some correlation with nondestructive MBN measurements indicating magnetic anisotropy have been shown. Since anisotropy is influenced by crystalline texture and residual stress the magnetic properties and effects of line pressure on MFL signals are dependent on the manufacturing processes for the particular line pipe.

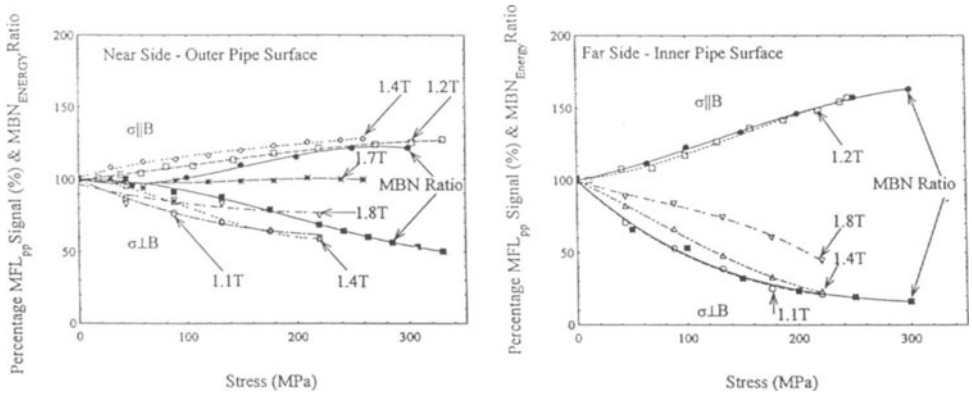

Fig. 9. Percentage MBN_{ENERGY} ratio, with respect to zero stress, and MFL_{pp} signals at various pipe wall axial flux densities, both for both axial and circumferential stresses as functions of stress for 13mm diameter 50% penetration ball-milled pits on near side (left) outer pipe surface and far side (right) inner pipe surface.

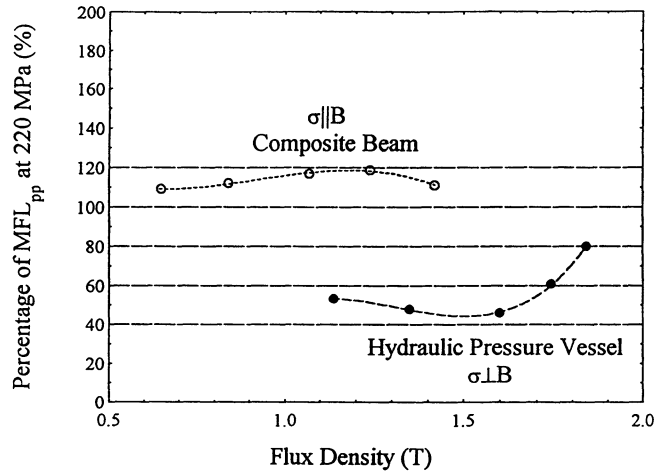

Fig. 10. Percentage of MFL_{pp} signals at 220MPa with respect to 0MPa from near side pits for parallel and perpendicular field and stress as functions of flux density.

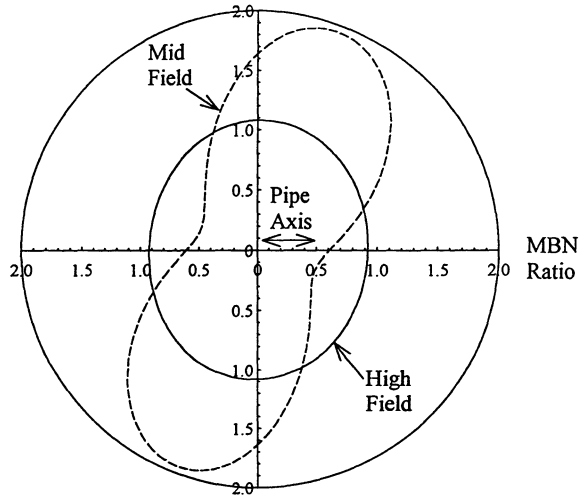

Fig. 11. Angular variation of the MBN_{ENERGY} ratio at 308MPa, normalized with respect to the 0MPa value, for circumferential stress at mid and higher fields.

ACKNOWLEDGEMENT

This research was supported by Gas Research Institute, Natural Sciences and Engineering Research Council of Canada and Pipetronix Ltd.

REFERENCES

1. D. L. Atherton, Oil & Gas J., Vol. 87, No. 32, 52-61 (1989).
2. C. Hauge and D.L. Atherton, Oil & Gas J., Vol. 94, No. 12, 92-96 (1996).
3. D.L. Atherton et al., Gas Research Institute Report # GRI-96-0197, (1996).
4. T.W. Krause et al., in press Research in Nondestructive Evaluation (1996).
5. A. Dhar et al., Materials Evaluation, Vol. 50, No. 10, 1139-1141 (1992).
6. T.W. Krause, L. Clapham and D.L. Atherton, J. Appl. Phys., Vol. 75, No. 12, 7983-7988 (1994).